Title

Prototyping the GMT phasing camera with the Magellan AO system

Permalink

https://escholarship.org/uc/item/81f1f8pt

Journal

Adaptive Optics for Extremely Large Telescopes 4 – Conference Proceedings, 1(1)

Authors

Kopek, Derek
McLeod, Brian
McCracken, Kenneth
et al.

Publication Date

2015

DOI

10.20353/K3T4CP1131566

Prototyping the GMT phasing camera with the Magellan AO system

Derek Kopon*[a], Brian McLeod[a], Kenneth McCracken[a], Marcos van Dam[b], Antonin Bouchez[c], Alan Conder[c], William Podgorski[a], Daniel Catropa[a], Stuart McMuldroch[a], Laird Close[d], Jared Males[d], Katie Morzinski[d], Timothy Norton[a]

[a]Harvard Smithsonian Center for Astrophysics, 60 Garden Street, Cambridge, MA 02138
[b]Flat Wavefronts, 21 Lascelles St., Christchurch 8022, New Zealand
[c]GMTO Corporation, 251 S. Lake Ave., Suite 300, Pasadena, CA, 91101
[d]Steward Observatory, University of Arizona, Tucson, AZ 85721

ABSTRACT

The future diffraction-limited performance of the 25.4 meter Giant Magellan Telescope (GMT) will rely on the active and adaptive wavefront sensing measurements made by the Acquisition, Guiding, and Wavefront Sensor (AGWS) currently being designed by SAO. One subsystem of the AGWS, the phasing camera, will be responsible for measuring the piston phase difference between the seven GMT primary/secondary segment pairs to 50 nm accuracy with full sky coverage using natural guide stars that are 6-10 arcmin off-axis while the on-axis light is used for science operations. The phasing camera will use a dispersed fringe sensor to measure the phase difference in rectangular subapertures spanning the gaps between adjacent mirror segments. The large gap between segments (>295 mm, compared to 3 mm for the Keck telescope) reduces the coherence of light across the subapertures, making this problem particularly challenging. In support of the AGWS phasing camera technical goals, SAO has undertaken a series of prototyping efforts at the Magellan 6.5 meter Clay telescope to demonstrate the dispersed fringe sensor technology and validate atmospheric models. Our latest on-sky test, completed in December 2015, employs a dual-band (I and J) dispersed fringe sensor. This prototype uses an adaptive optics corrected beam from the Magellan AO adaptive secondary system. The system operates both on-axis and 6 arcmin off-axis from the natural guide star feeding the MagAO wavefront sensor. This on-sky data will inform the development of the AGWS phasing camera design towards the GMT first light.

Keywords: Active optics, adaptive optics, Giant Magellan Telescope, phasing, dispersed fringe sensor

1. INTRODUCTION

The Giant Magellan Telescope (GMT) is a 25.4 meter diameter telescope that will consist of seven 8.4 meter diameter primary mirror segments, each of which corresponds to a 1 meter diameter adaptive mirror of a segmented secondary[1]. Reaching the GMT's diffraction limit during adaptive optics operation will require phasing each primary-secondary pair to a fraction of the observing wavelength[2]. While other telescopes with segmented primary mirrors have been successfully phased in the past[3], the GMT phasing problem is uniquely difficult for several reasons. The minimum primary mirror segment gap is 295 mm between outer segments and 359 mm between the inner and outer segments, compared to ~3mm for the Keck telescope[4]. This large segment gap requires the phasing sensor to use a longer wavelength of light in order to maintain acceptable phase coherence. An earlier SAO phasing sensor prototype operating in the K-band was operated at the Magellan telescope in 2012[5]. Recent simulations by Van Dam suggest that a dispersed fringe sensor capable of operating in J-band should meet the GMT requirements for capture range, sensitivity, and sky coverage[6]. While current commercially available detectors do not have sufficient low-noise sensitivity in the J-band, recent advances with Avalanche Photodiode Detectors (e-APD) may make this a possibility[7]. The GMT phasing problem is further complicated by the segmented secondary. Having both a segmented primary and a segmented secondary creates degeneracies in segment tip/tilt and off-axis piston.

---

* derek.kopon@cfa.harvard.edu

The AGWS is a multi-purpose sensor package containing movable star probes that acquire natural guide stars for a number of purposes during commissioning and science operation[8]. The AGWS will be responsible for guiding, primary mirror active optics, primary/secondary tip/tilt control, ground layer wavefront sensing, and primary/secondary segment phasing. Our prototyping efforts focus on the phasing capability of the AGWS. For more on the other functions of the AGWS, see McLeod et al 2014.

The baseline design for the phasing sensor is a dispersed fringe sensor[9]. The phasing sensor must be able to operate during Laser Tomographic Adaptive Optics (LTAO) mode, which will require the use of off-axis guide stars while the on-axis light is used for science operations. The off-axis guide stars in an annular patrol field of 6-10 arcmin will be aberrated by the telescope, requiring a phasing sensor capable of operating off-null on natural guide stars on a curved focal plane. During NGS operation, when bright guide stars are available at or near the center of the science field, the GMT science instruments will have their own on-board wavefront sensors capable of the keeping the telescope phased. The current baseline for these on-board on-axis sensors is a pyramid wavefront sensor.

2. THE PHASING PROTOTYPE

The SAO prototype operating in conjunction with the Magellan AO system provides the opportunity to verify the dispersed fringe phasing technology on sky behind a high order AO system running in closed loop[10]. The prototype is designed to mount to the telescope at one of two distinct locations: either on-axis, or 6 arcmin off-axis. 6 arcmin is the same off-axis distance of the inner edge of the GMT phasing sensor annular patrol field and will allow us to verify simulations and the atmospheric structure function at the same off-axis distance.

The GMT phasing sensor design will use an e-APD detector that provides low read noise (<1 e-) and fast read out (max ~3500 fps). Because such detectors are not yet on the market, we designed the prototype to work in two different wavelength bands: I-band using a readily available fast low read-noise EMCCD, and J-band with an InGaAs detector in order to operate at the same wavelength as the GMT baseline. The Ninox 640 InGaAs camera we selected provides fast readout, but lower sensitivity and higher read noise (50 electrons) than the e-APD detector will, when it becomes available. As a result of this, the prototype will use bright target stars in J-band and fainter stars in the I-band.

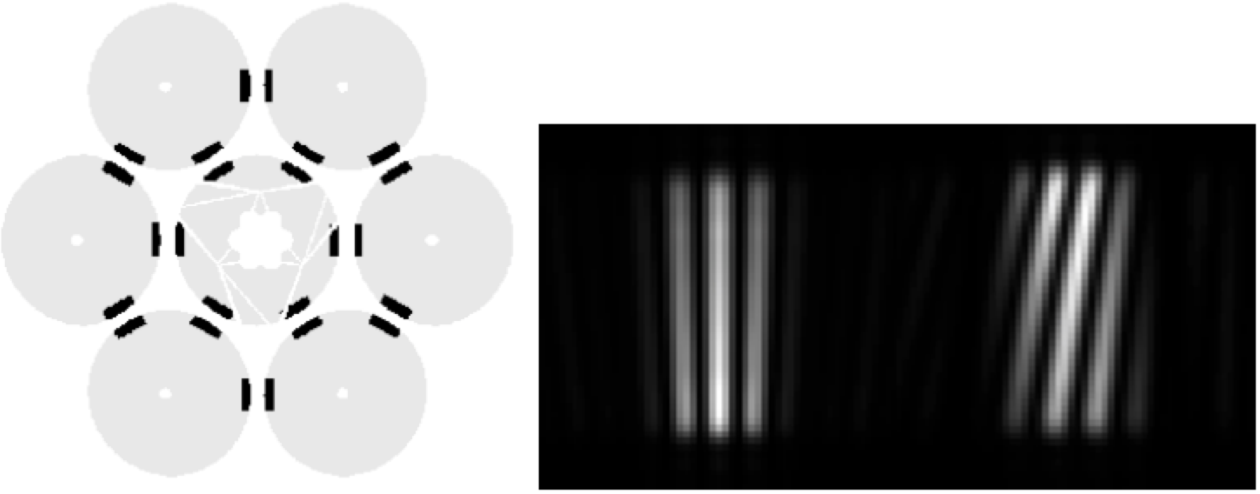

Figure 1: Left: Diagram of the GMT pupil overlaid with the segment boundary aperture mask. The 12 pairs of subapertures will form 12 dispersed fringe patterns that provide segment phasing data. Right: Simulated fringes from one subaperture showing 0 piston phase difference (left) and 10 microns (right).

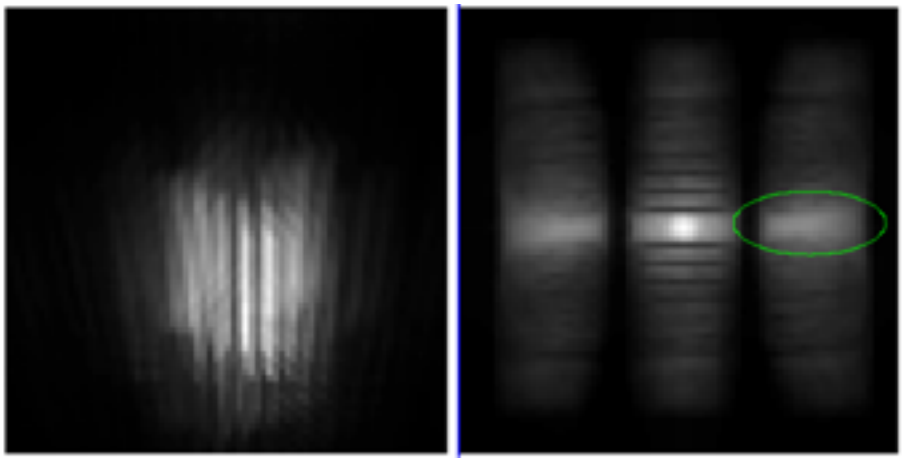

Figure 2: Simulated dispersed fringe image and its FFT. The vertical position of the circled peak determines the tilt of the fringes and therefore the piston error[11].

3. OPTICAL DESIGN

The phasing prototype optical design consists of two wavelength channels: I band and J band. Each wavelength channel has an imaging mode that produces 6 dispersed fringe PSFs and a pupil viewing mode that images the 6 pairs of subapertures within the Magellan pupil.

3.1 I-band channel

The focal lengths and beam diameters of the I-band channel are largely driven by the selection of available catalogue hexagonal lenslet arrays. A custom lenslet array could not be considered because of the accelerated schedule. A lens located after the Magellan F/16 focus collimates the beam and reimages the pupil onto a laser cut aperture mask containing 6 pairs of GMT segment boundaries designed to fit within the Magellan pupil (Fig. 3). The mask is followed closely by the lenslet array. Shortly thereafter follows the I-band grism, which is made from a stock Thorlabs prism with a Richardson replicated grating. After the grism is an intermediate focus followed by a two lens optical relay and I-band filters. Because the optimal design wavelengths (760-900 nm) differ slightly from the canonical astronomical I-band (730-880 nm), we use a long-pass filter and a short-pass filter in combination as an efficient and economical way of selecting our desired wavelengths. The last lens in the optical train, L3, is mounted on a stage that allows it to be removed from the beam and replaced with a different pair of lenses capable of creating a pupil image on the detector (Fig. 4). The pupil imaging mode is valuable for aligning the system internally and to the telescope. The pupil mode is also used to ensure uniform illumination over all of the subapertures.

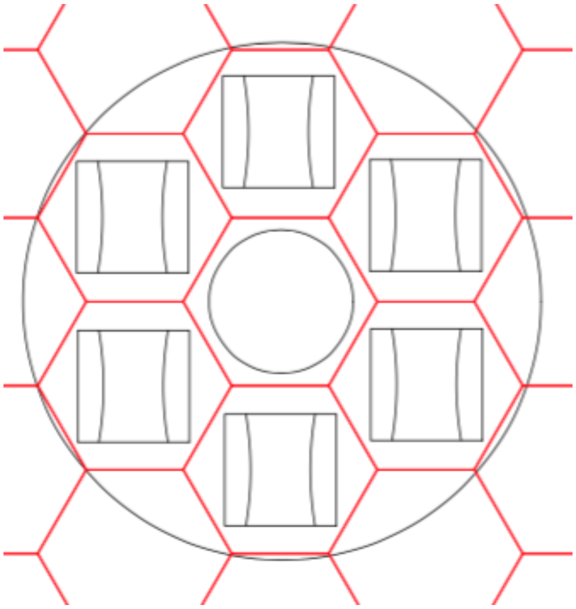

Figure 3: Subaperture mask and hexagonal lenslet array superimposed on the pupil of the 6.5 meter Magellan primary.

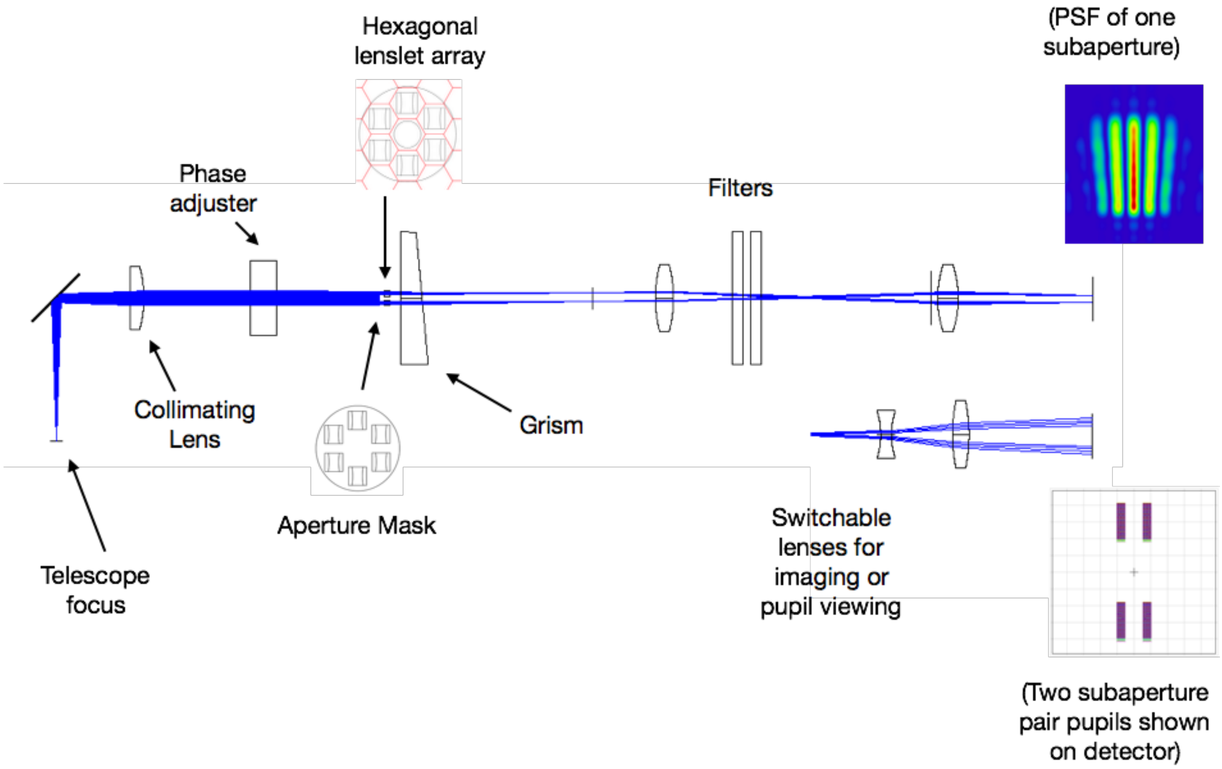

Figure 4: Optical ray trace of the I-band channel.

3.2 J-band channel

The J-band optical design uses the same collimating lens as the I-band channel and a similar lenslet/mask assembly (the only difference being the AR coating on the lenslet array). The J-band channel uses a different grism whose apex angle and grating prescription have been chosen to give optimal performance at the different band. The relay optics downstream operate similarly to the I-band design and provide imaging and pupil viewing modes (Fig. 5).

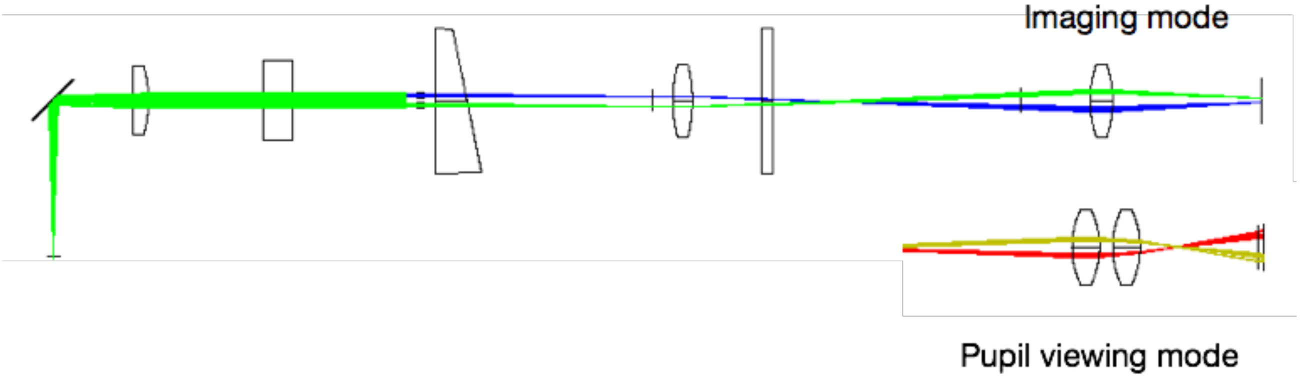

Figure 5: The J-band optical design. Prior to the grism, the optics are the same as the I-band design.

3.3 Phase shifting

We place a phase shifter in the beam following the collimating lens in order to induce a phase shift across a subaperture pair similar to what we would see across a GMT segment boundary between two segments with non-zero piston phase difference. The phase adjuster consists of two plane parallel AR-coated BK7 rectangular windows of equal thickness, each covering half of the telescope pupil. One of the phase pieces is stationary, the other can be rotated an arbitrary amount. By rotating the glass, the path length of glass in the beam is increased, thereby introducing a phase shift (Fig. 6). The phase shifter gap intersects the top and bottom subaperture pairs, providing two sets of phase shifted fringes.

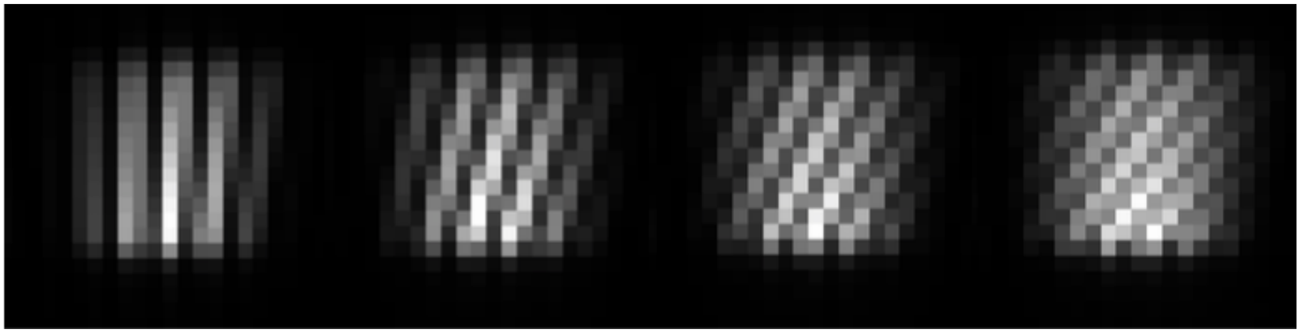

Figure 6: Simulated fringes with phase difference of 0, 5, 10, 15 microns. Figure taken from van Dam et al. 2015.

3.4 Off-axis design

On the GMT, the phasing camera will patrol an annular acquisition field from 6-10 arcmin, with a goal of 3-10 arcmin. In order to replicate this configuration, we designed the prototype to also work at 6 arcmin off-axis on the Magellan telescope. Unlike the GMT, which is a coma-free aplanatic Gregorian, the Magellan telescopes have significant coma and astigmatism off-axis. In our case, the aberrations at 6 arcmin off-axis would be large enough to reduce fringe contrast and add spurious phase shifts to some subapertures. To correct these aberrations, we designed an off-axis lens assembly (OAL) to cancel the static telescope aberrations at 6 arcmin. The OAL consists of three off-the-shelf singlets that are precisely tilted and decentered to cancel the telescope aberrations at only this single off-axis location (Fig. 7). When the prototype is moved to 6 arcmin off-axis, the OAL can be placed in the beam, replacing the phase shifter. The same OAL can operate in both the I and J band channels.

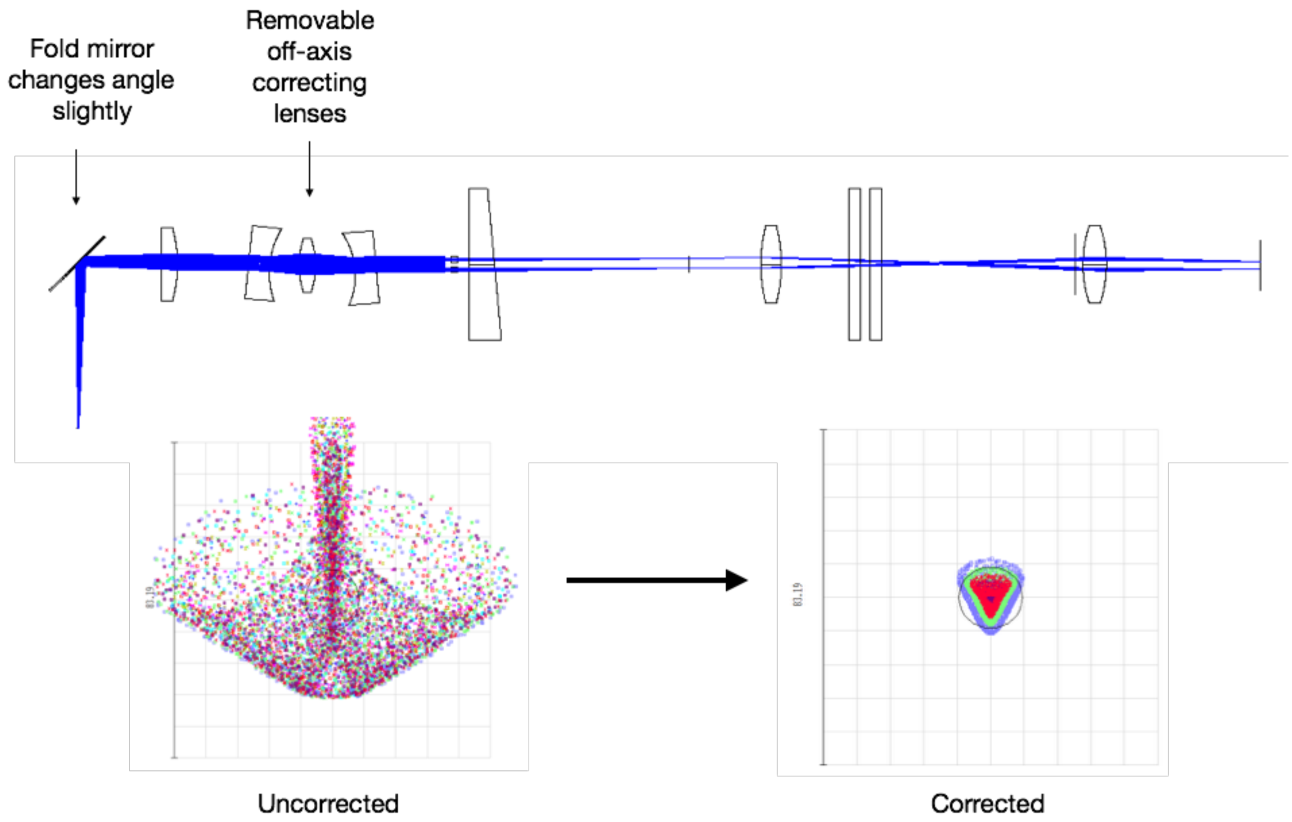

Figure 7: The 3-element off-axis lens assembly in the I-band optical path. The same OAL is used for both the I and J band channels. The OAL assembly improves the rms spot size from 22.5 mas (left) to 2.38 mas (right).

4. INSTRUMENT DESIGN

The phasing prototype mounts to a plate on the nasmyth platform of the Magellan Clay telescope. A beamsplitter in front of the prototype field stop sends a reflected beam to the MagAO wavefront sensor, which is always on-axis. The transmitted beam from the beamsplitter passes through a 3 arcsec field stop in the prototype and is then reflected off of an adjustable fold mirror to the collimating lens. The field outside of the 3 arcsec hole out to ~25 arcsec is reflected by a fold flat to a Stellacam acquisition camera.

The prototype contains several manually actuated stages that can be used to select between channels and observing modes (Fig. 8). The instrument is mounted to a sled that can translate between hard stops at the on-axis position and 6 arcmin off-axis. The collimating lens after the field stop is fixed and common to both I and J-band channels. After this lens, a stage with three positions can be used to insert either the phase shifter, the OAL assembly, or nothing into the beam. After this stage, a larger stage can be used to select either the I or J band channels, each of which has its own optics from the aperture mask on that are stationary with respect to its detector. Each wavelength channel has a smaller slide just before the detector that can be used to select the imaging or pupil viewing optics.

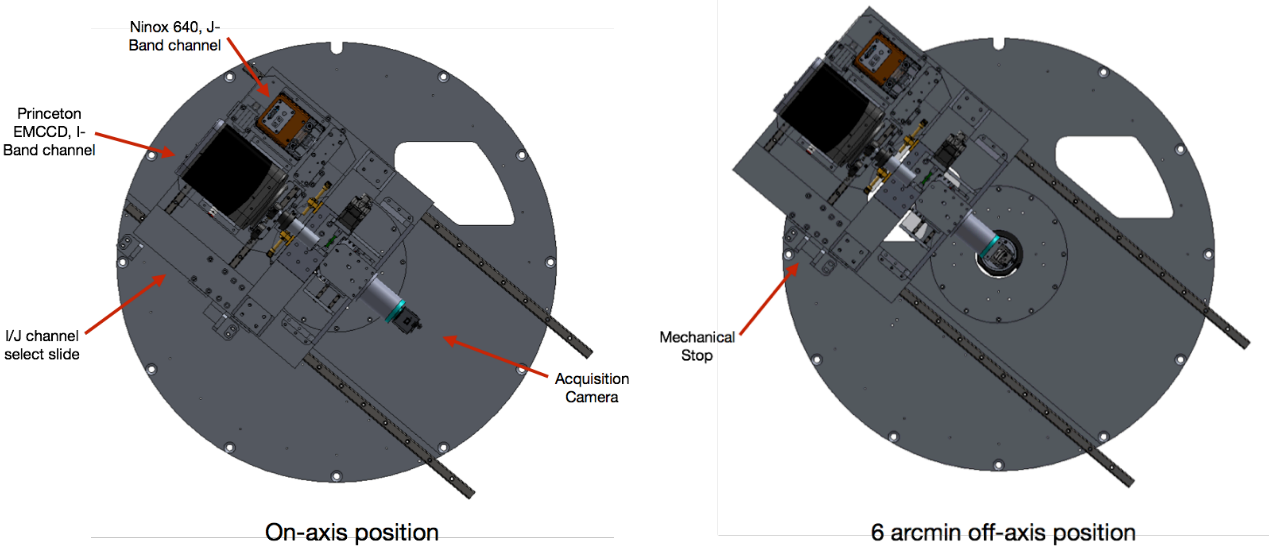

Figure 8: CAD model of the prototype on the nasmyth mounting plate. There are three detectors: the Stellacam acquisition camera that views a ~25" FOV outside of the 3" field stop, the I-band Princeton EMCCD, and the J-band Ninox 640 InGaSa detector. Various manual slides are used to select between off-axis position, wavelength channel, phase shifter in or out of beam, off-axis correcting lenses, and imaging/pupil mode. Prototype is shown on-axis (left) and at 6 arcmin off-axis (right).

5. LAB TESTS

The prototype was mounted to a jig plate attached to an optical table in order to simulate the same gravity orientations that the instrument will see at the Nasmyth platform of the telescope (Fig. 9). Two light sources were used for lab testing the instrument. The first is the on-board calibration source consisting of a light bulb and an optical diffusing plate behind a pinhole. The other is a similar point source located on the bench that is reimaged to the instrument field stop using two relay lenses (Fig. 10). The bench source has the benefit of having an easily accessible focal plane for various pinholes and flat-field targets, in addition to having a collimated beam where a turbulence phase generator can be located. We use a rotating Lexitech phase screen with the focal length of the collimator chosen to match the phase screen r_o to that of the LCO site. The laboratory results demonstrate good agreement with the simulations, with a slight loss in contrast most likely due to the finite extent of the resolved pinhole. I-band laboratory fringes are shown in Figure 11.

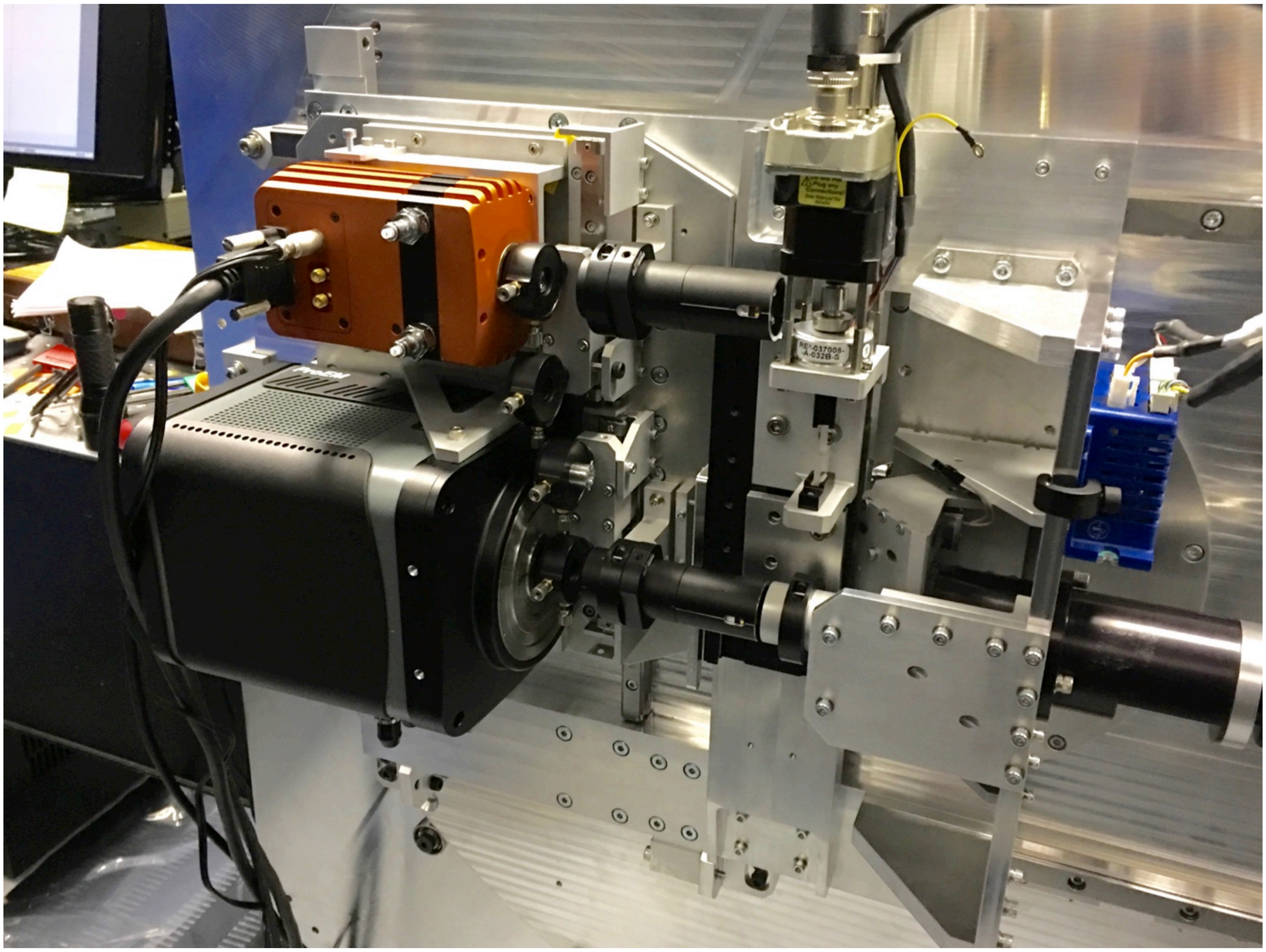

Figure 9: The prototype mounted to the jig plate in the lab in a horizontal position. The instrument was then shipped fully assembled to Chile.

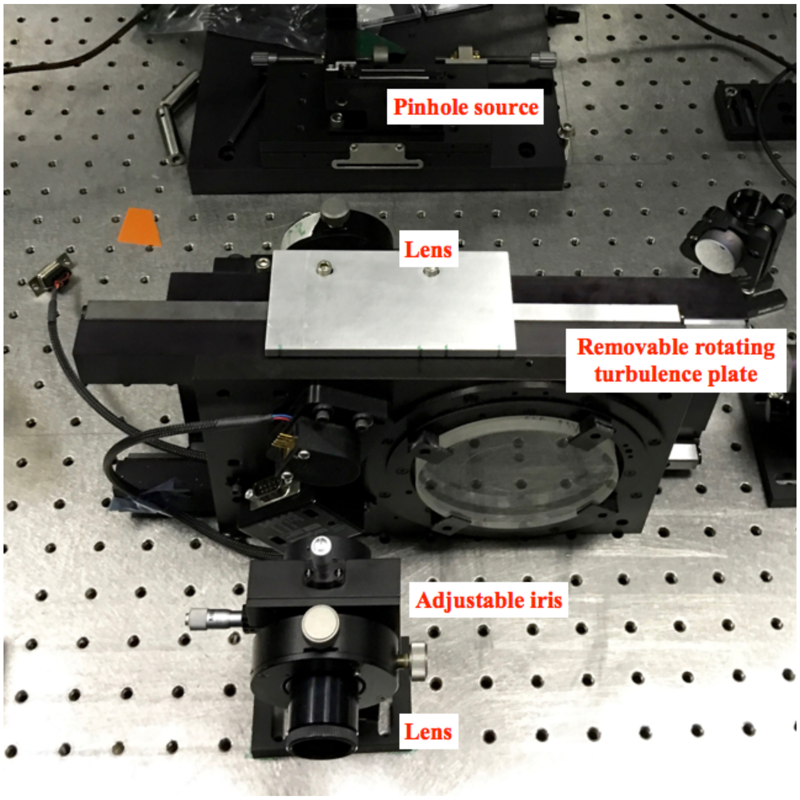

Figure 10: Photo of the bench calibration source and optics. The source is at the top of the photo, the field stop entrance to the instrument is fed by the lens at the bottom of the picture.

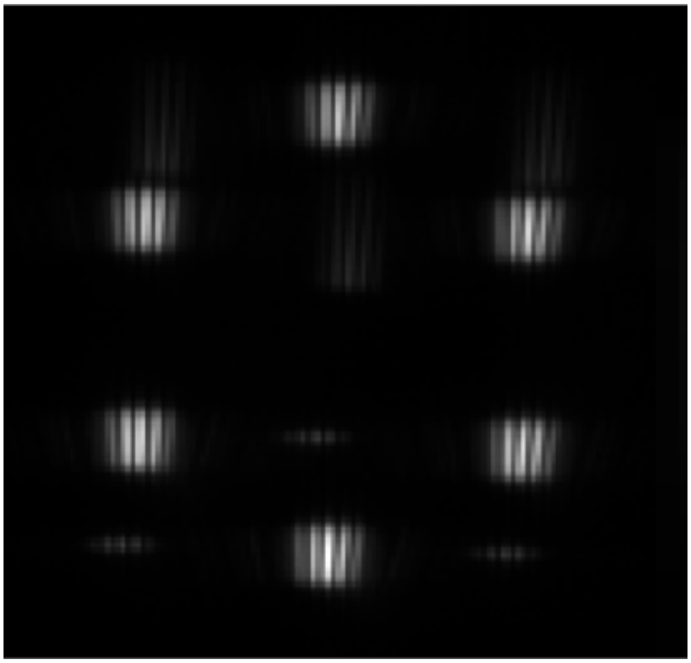

Figure 11: Laboratory I-band fringes from the 6 sets of segment subaperture pairs. Fainter 0th and 2nd order sets of fringes can also be seen.

CONCLUSION

We have designed and built a prototype dispersed fringe sensor for the Magellan telescope that will demonstrate on-sky the technology that will be used to measure piston phase difference between the seven GMT primary/secondary segment pairs. Our prototype operates behind the Magellan AO system, which is a high-order adaptive secondary system, similar to what will be deployed on the GMT. Our prototype operates both on-axis and at 6 arcmin off-axis, which will be the minimum patrol field radius at the GMT. The prototype has two wavelength channels: an I-band channel that uses an EMCCD, and a J-band channel that uses an InGaAs detector. We commissioned the prototype during three nights at the telescope in December 2015, results from that run will be presented in a future paper.

Acknowledgements

This work was supported by the GMTO Corporation, a non-profit organization operated on behalf of an international consortium of universities and institutions: Astronomy Australia Ltd., the Australian National University, the Carnegie Institution for Science, Harvard University, the Korea Astronomy and Space Science Institute, The Sao Paolo Research Foundation, the Smithsonian Institution, The University of Texas at Austin, Texas A&M University, University of Arizona, and University of Chicago.

REFERENCES

[1] Bouchez, A. H., Acton, D. S., Biasi, R., Conan, R., Espeland, B., Esposito, S., Filgueira, J. M., Gallieni, D., McLeod, B. A., et al., “The Giant Magellan Telescope adaptive optics program,” Proc. SPIE **9148**, 91480W – 91480W – 19 (2014).

[2] Codona, J., “Pairwise Segment Phasing with the GMT” (2008), internal design report.

[3] Albanese, M., Wirth, A., Jankevics, A., Gonsiorowski, T., Ohara, C., Shi, F., Troy, M., Chanan, G.., Acton, S., “Verification of the James Webb Space Telescope coarse phase sensor using the Keck Telescope,” Proc. SPIE

6265, 62650Z – 62650Z – 9 (2006).

[4] Bouchez, A. H., McLeod, B. A., Acton, D. S., Kanneganti, S., Kibblewhite, E. J., Shectman, S. A.., van Dam, M. A., "The Giant Magellan Telescope phasing system," Proc. SPIE **8447**, 84473S – 84473S – 9 (2012).

[5] Kanneganti, S., McLeod, B. A., Ordway, M. P., Roll, J. B., Shectman, S. A., Bouchez, A. H., Codona, J., Eng, R., Gauron, T. M., et al., "A prototype phasing camera for the Giant Magellan Telescope," Proc. SPIE **8447**, 844710–844752 (2012).

[6] van Dam, M. A., McLeod, B. A.., Bouchez, A. H., "Dispersed fringe sensor for the Giant Magellan Telescope," Appl. Opt. **55**(3), 539–547, OSA (2016).

[7] Feautrier, P., Gach, J.-L.., Wizinowich, P., "State of the art IR cameras for wavefront sensing using e-APD MCT arrays," AO4ELT4 (2015), these proceedings.

[8] McLeod, B., Bouchez, A. H., Espeland, B., Filgueira, J., Johns, M., Norton, T. J., Ordway, M., Podgorski, W. A., Roll, J., et al., "The Giant Magellan Telescope active optics system," Proc. SPIE **9145**, 91451T – 91451T – 13 (2014).

[9] Shi, F., Chanan, G., Ohara, C., Troy, M.., Redding, D. C., "Experimental verification of dispersed fringe sensing as a segment phasing technique using the Keck telescope," Appl. Opt. **43**(23), 4474–4481, OSA (2004).

[10] van Dam, M.., McLeod, B. A., "FWN 76: Design of AGWS Phasing Sensor Prototype" (2015), internal design report.

[11] McLeod, B. A.., Close, L. M., "AGWS Phasing Proposal" (2015), internal design report.